

# Fluctuation of Voids in Hadronization at Phase Transition

Rudolph C. Hwa and Qing-hui Zhang  
Institute of Theoretical Science and Department of Physics  
University of Oregon, Eugene, OR 97403-5203

## Abstract

Starting from the recognition that hadrons are not produced smoothly at phase transition, the fluctuation of spatial patterns is investigated by finding a measure of the voids that exhibits scaling behavior. The Ising model is used to simulate a cross-over in quark-hadron phase transition. A threshold in hadron density is used to define a void. The dependence of the scaling exponents on that threshold is found to provide useful information on some properties of the hadronization process. The complication in heavy-ion collision introduces the possibility of configuration mixing, which can also be studied in this approach. Numerical criteria on the scaling exponents have been found that can be used to discriminate phase-transition processes from other hadronization processes having nothing to do with critical phenomena.

## 1 Introduction

One of the generic properties of second-order phase transition is clustering. In the case of a magnetic system, it means that there are regions of all sizes, in which spins point in the same direction, and that the probability of having a cluster of a certain size satisfies a scaling law. The implication of those properties for quark-hadron phase transition (PT) is that hadronization does not occur uniformly at the critical temperature ( $T_c$ ). At any instant during the entire course of the hadronization process of a quark-gluon plasma system, there are then clusters of hadrons separated by regions of no hadrons. In the case of heavy-ion collisions it is the surface of the expanding cylinder that is around  $T_c$ , and the clusters are to appear on the two-dimensional cylindrical surface. We call the non-hadronic regions between the clusters voids. To detect voids will be a sign of the second-order PT. In this paper we study the properties of the voids and discuss how to identify their properties in heavy-ion experiments.

It should be understood that voids are not frozen on a plasma surface for all times. If one could take instantaneous pictures of the cylindrical surface at time intervals of 1 fm/c apart, one would see the clustering patterns to fluctuate from picture to picture. Simulation on a 2D lattice using the Ising model shows that at  $T_c$  the clustering patterns differ from one configuration to another. An example of the clusters of hadrons formed can be seen in Fig. 2 of Ref. [1]. There are regions of high hadron density, low hadron density, and no hadrons. A region without hadrons (i.e. a void) consists of quarks and gluons in the

deconfined state at a particular instant in time; they are likely to form hadrons a little later in the evolution process. The reason for the voids to exist is that at the critical point the system is torn between being in the ordered state of confinement and the disordered state of deconfinement. It is this tension of coexistence of the two states at  $T_c$  that is responsible for the many interesting behaviors of critical phenomena [2]. Thus if the plasma volume created in a heavy-ion collision is hot in the interior and cools to  $T_c$  on the surface, a second-order PT, which is assumed here, would imply that the hadrons are not produced smoothly in time or space. Whereas hadronic clusters in the  $\eta$ - $\phi$  space may be hard to quantify, voids are relatively easy to define, though not trivially. Our first problem will be to characterize the voids. To identify them in the theoretical laboratory is, however, much simpler than to find them in the experimental data. The latter problem will also be addressed in this paper.

A simple way to appreciate voids is to examine the exclusive distribution in rapidity space for a hadronic collision process. Since the rapidity of each produced particle can be precisely determined, one can calculate the rapidity gaps between each pair of neighboring particles. Those rapidity gaps are the 1D version of the voids in 2D. An extensive consideration of the properties of gaps in hadronic processes is given in Ref. [3]. Although it is easy to gain a mental picture of gaps in hadronic collisions, it is nontrivial to define a measure of voids in heavy-ion collisions, in which the hadronization process extends over a long period of time.

To gain some physical insight into the fluctuation phenomenon in particle production at the critical point, it is helpful to consider the production of photons at the threshold of lasing. The physics of single-mode lasers being completely understood, their operation near the threshold is known to behave as in a second-order PT [4]. When the pump parameter is set at the threshold of lasing, the system does not continuously produce photons as a function of time. The photons are produced in spurts with gaps of quiescence between spurts. Such fluctuations have been measured and the result in terms of factorial moments [5] agree with the prediction based on the Ginzburg-Landau description of PT [6]. Those gaps in the time series in the photo-count problem are similar to the voids in the hadron-count problem in heavy-ion collisions. Since lattice QCD cannot be applied efficiently to the simulation of spatial patterns in the PT problems, we make use of the universal features of the Ginzburg-Landau theory and, in particular, employ the 2D Ising model to simulate the hadronic clusters in the  $\eta$ - $\phi$  plane. This approach to the problem was initiated in [7], where the scaling properties of cluster production were examined. More recently, an effort was made to find observable critical behavior in quark-hadron PT [1]. Here, we use the same formalism to study the properties of voids and search for observable measures that can signal PT in heavy-ion collisions.

## 2 Hadron Production in the Ising Model

It is known through studies in lattice QCD that the nature of the phase transition depends on the number of flavors and the quark masses [8]. For  $m_u = m_d = 0$ , the PT is first-order for low  $m_s$ , but second-order at high  $m_s$ . For nonzero  $m_u$  and  $m_d$ , the former region remains first-order (but for even smaller values of  $m_s$ ), while the latter region of high  $m_s$  becomes a cross-over. The two regions are separated by a phase boundary that is second-order and has possibly the Ising critical exponents [9]. For realistic quark masses we are probably in the

region of the cross-over, which is what we shall assume in this study.

A cross-over means that no calculable or measurable quantities and their derivatives undergo any discontinuity as  $T$  is varied across  $T_c$ . In the 2D Ising model the situation is like having a small external magnetic field so that the average magnetization of the system varies smoothly across  $T_c$ . The phase diagrams of the order parameter versus  $T$  are very similar for the Ising model and the QCD problem. Since lattice QCD is so much more difficult to study compared to the Ising model, we shall hereafter concentrate only on the use of the Ising model to simulate hadron production.

Following the formalism already described in Refs. [1, 7] let us briefly summarize how hadron density is defined on the Ising lattice in 2D. For a lattice of size  $L \times L$  with each site having spin  $\sigma_j$ , we define the spin aligned along the overall magnetization  $m_L = \sum_{j \in L^2} \sigma_j$  by

$$s_j = \text{sgn}(m_L) \sigma_j \quad (1)$$

where  $\text{sgn}(m_L)$  stands for the sign of  $m_L$ . We then define the spin of a cell of size  $\epsilon \times \epsilon$  at location  $i$  by

$$c_i = \sum_{j \in A_i} s_j \quad (2)$$

where  $A_i$  is the cell block of  $\epsilon^2$  sites at  $i$ . Since  $c_i$  averages over all site spins in a cell, it should approach zero at high  $T$  for which the system is in a disordered state, and should approach  $\epsilon^2$  as  $T \rightarrow 0$  for which the system is in an ordered state. Note that even in the absence of an external magnetic field,  $c_i$  approaches  $+\epsilon^2$  at low  $T$ , never  $-\epsilon^2$ , because of our definition of  $s_j$ . Thus unlike the average magnetization  $\langle m_L \rangle$  of the usual Ising model without external field, which is zero for all  $T > T_c$ , the average cell spin  $\langle c_i \rangle$  varies smoothly from high to low  $T$ , similar to the behavior of  $\langle m_L \rangle$  in the presence of external field.

The hadron density, being proportioned to the order parameter, can now be defined as

$$\rho_i = \lambda c_i^2 \theta(c_i) \quad , \quad (3)$$

where  $\lambda$  is an unspecified factor relating the lattice spins to the number of particles in a cell. In any configuration  $c_i$  may still fluctuate from cell to cell. We identify only the positive  $c_i$  cells with hadron formation, and associate the hadron density with  $c_i^2$ , just as the order parameter in the Ginzburg-Landau formalism is associated with the square of the Ising spins [2]. If  $\langle \rho \rangle$  denotes the average density, i.e.,  $\rho_i$  averaged over all cells on the lattice and over all configurations, then the dependence of  $\langle \rho \rangle$  on  $T$  is as shown in Fig. 1. It is typical of a cross-over, shown in Fig. 1 of Ref. [9] for small quark masses. The essence of that dependence is that  $\langle \rho \rangle$  decreases precipitously but smoothly, as  $T$  is increased across  $T_c$ , but remains nonzero for a range of  $T$  above  $T_c$ . Evidently, we have succeeded in simulating a cross-over without the explicit introduction of an external field in the Ising Hamiltonian

$$H = -J \sum_{\langle ij \rangle} \sigma_i \sigma_j \quad . \quad (4)$$

Since the dependence of  $\langle \rho \rangle$  on  $T$  is smooth, it is a nontrivial problem to determine the precise value of  $T_c$ . That has been done in Ref. [7] by examining the scaling behavior of

the normalized factorial moments  $F_q$ . It is found that  $F_q$  behaves as  $M^{\varphi_q}$  only at  $T = 2.315$  (in units of  $J/k_B$ ), where  $M$  is the number of bins on the lattice. Since the critical point is characterized by the formation of clusters of all sizes in a scale independent way, we identify the critical temperature at  $T_c = 2.315$ . Indeed, it has been shown in Ref. [1] that in the neighborhood of  $T_c$  with  $T \leq T_c$ ,  $\langle \rho \rangle$  behaves as

$$\langle \rho \rangle - \langle \rho_c \rangle \propto (T_c - T)^\eta, \quad \eta = 1.67 \quad , \quad (5)$$

where  $\langle \rho_c \rangle$  is  $\langle \rho \rangle$  at  $T_c$ . There exist other measures that exhibit critical behaviors,  $(T_c - T)^{-\zeta}$ , with negative exponents. They are discussed in [1].

### 3 Scaling Behavior of Voids

We choose to work with a lattice having  $L = 256$  and cells having  $\epsilon = 4$ . Thus the total number of cells on the lattice is  $N_c = (L/\epsilon)^2 = 64^2$ . We divide the lattice into bins of size  $\delta^2$  so that each bin can contain  $\nu = (\delta/\epsilon)^2$  cells and the lattice can contain  $M = (L/\delta)^2$  bins. The average density of hadrons in a bin is therefore

$$\bar{\rho}_b = \frac{1}{\nu} \sum_{i=1}^{\nu} \rho_i \quad , \quad (6)$$

where  $b$  denotes the  $b$ th bin. Near  $T_c$ ,  $\bar{\rho}_b$  fluctuates from bin to bin, especially for small  $\delta$ . We define a bin to be “empty” when

$$\bar{\rho}_b < \rho_0 \quad , \quad (7)$$

where  $\rho_0$  is a floor level greater than zero. This criterion is chosen to eliminate the effect of small fluctuations on gross behavior. That is, for the purpose of defining a void, hadron clusters are counted only when the hadron density is above a threshold  $\rho_0$ . Bins with very low hadron density, i.e., where (7) holds, are then regarded as empty. A void is a contiguous collection of empty bins. Fig. 2 illustrates a pattern of voids in a configuration generated at  $T_c$  for  $M = 24^2$  and  $\rho_0 = 20$  (in units of  $\lambda$ ). An open square indicates an empty bin, while a black square contains hadrons with  $\bar{\rho}_b \geq \rho_0$ . In that configuration there are 26 voids, the sizes of which are 76, 35, 9, 8, 7,  $\dots$  in descending order. It should be recognized that the maximum hadron density that a cell can have is  $\rho_{\max} = (\epsilon^2)^2 = 256$ , so  $\rho_0 = 20$  represents a threshold that is less than 8% of the maximum.

Let  $V_k$  be the size of the  $k$ th void (in units of bins). That is, let

$$V_k = \sum_{\langle b \rangle_k} \theta(\rho_0 - \bar{\rho}_b) \quad , \quad (8)$$

where  $\langle b \rangle$  implies a sum over all empty bins that are connected to one another by at least one side;  $k$  simply labels a particular void. We can then define  $x_k$  to be the fraction of bins on the lattice that the  $k$ th void occupies:

$$x_k = V_k/M. \quad (9)$$

For each configuration we thus have a set  $\mathcal{S} = \{x_1, x_2, \dots\}$  of void fractions that characterizes the spatial pattern.

Since the pattern fluctuates from configuration to configuration,  $\mathcal{S}$  cannot be used to compare patterns in an efficient way. For a good measure to facilitate the comparison, let us first define the moments  $g_q$  for each configuration

$$g_q = \frac{1}{m} \sum_{k=1}^m x_k^q \quad , \quad (10)$$

where the sum is over all voids in the configuration, and  $m$  denotes the total number of voids. We then define the normalized  $G$  moments

$$G_q = g_q / g_1^q \quad , \quad (11)$$

which depends not only on the order  $q$ , but also on the total number of bins  $M$ . Thus by definition  $G_0 = G_1 = 1$ . This  $G_q$  is defined in the same spirit as that in [3] for rapidity gaps, but they are not identical because the  $x_k$  here for voids do not satisfy any sum rule. It is also unrelated to the  $G$  moments defined earlier [10] for fractal analysis. Now,  $G_q$  as defined in Eq. (11) is a number for every configuration for chosen values of  $q$  and  $M$ . With  $q$  and  $M$  fixed,  $G_q$  fluctuates from configuration to configuration and is our quantitative measure of the void patterns, which in turn are the characteristic features of phase transition.

In Fig. 3 we show the probability distribution of  $G_q$  for  $q = 6$  and  $M = 36^2$  and  $\rho_0 = 20$  at three different values of  $T$ . The Wolff algorithm has been used in the Monte Carlo simulation to reduce the correlation between configuration [2, 11]. The distribution in Fig. 3 and other quantities to be calculated below are the results obtained using  $5 \times 10^3$  uncorrelated configurations. Since the value of  $G_q$  fluctuates widely from configuration to configuration covering a range that exceeds 3 orders of magnitude, we have plotted the distribution in  $\ln G_q$ . Since both the mean and the dispersion of  $\ln G_q$  shown in Fig. 3 vary significantly with  $T$ , and with  $q$  and  $M$  not shown in Fig. 3, it is necessary for us to search for simple regularities in the nature of the fluctuations of  $G_q$ .

Our first step in that search is to study the  $M$  dependence of the average of  $G_q$  over all configurations, i.e.,

$$\langle G_q \rangle = \frac{1}{\mathcal{N}} \sum_{e=1}^{\mathcal{N}} G_q^{(e)} \quad , \quad (12)$$

where the superscript  $(e)$  denotes the  $e$ th event (or configuration) and  $\mathcal{N}$  is the total number of events. In Fig. 4 we show  $\langle G_q \rangle$  versus  $M$  in a log-log plot for  $T = T_c$ ,  $2 \leq q \leq 8$ , and  $\rho_0 = 20$ . We find very good linear behavior; consequently, we may write

$$\langle G_q \rangle \propto M^{\gamma_q} \quad . \quad (13)$$

This scaling behavior implies that voids of all sizes occur at PT. Since the moments at different  $q$  are highly correlated, we expect the scaling exponent  $\gamma_q$  to depend on  $q$  in some simple way. Fig. 5 shows the dependence of  $\gamma_q$  on  $q$ , and we find remarkable linearity. Thus we may write

$$\gamma_q = c_0 + c q \quad , \quad (14)$$

where  $c = 0.8$ . There is no obvious reason why the  $q$ -dependence of  $\gamma_q$  should be so simple. We should regard (14) only as a convenient parameterization of  $\gamma_q$  that allows us to focus on  $c$  as a numerical description of the scaling behavior of the voids at PT.

It is evident from Fig. 3 that studying the behavior of  $\langle G_q \rangle$  extracts only a limited amount of information about the distribution  $P(G_q)$ . The fluctuation of  $G_q$  from event to event can be quantified by the various moments of  $G_q$

$$C_{p,q} = \frac{1}{N} \sum_{\epsilon=1}^N (G_q^{(\epsilon)})^p = \int dG_q G_q^p P(G_q) \quad , \quad (15)$$

among which  $\langle G_q \rangle$  corresponds only to  $C_{1,q}$ . Instead of examining a collection of  $C_{p,q}$  for various values of  $p$ , we consider the derivative of  $C_{p,q}$  at  $p = 1$  [3, 12], and define

$$S_q = \left. \frac{d}{dp} C_{p,q} \right|_{p=1} = \langle G_q \ln G_q \rangle \quad , \quad (16)$$

where  $\langle \dots \rangle$  stands for averaging over all configurations. Despite its appearance,  $S_q$  is not entropy, but is a measure of the fluctuations of  $G_q$ , when compared with  $\langle G_q \rangle \ln \langle G_q \rangle$ .

In Fig. 6 we show the power-law behavior of  $S_q$  at  $T_c$

$$S_q \propto M^{\sigma_q} \quad , \quad (17)$$

where the scaling exponents  $\sigma_q$  are the slopes of the straight lines in the figure. Because of Eq.(13),  $\langle G_q \rangle \ln \langle G_q \rangle$  is not power behaved, so  $S_q - \langle G_q \rangle \ln \langle G_q \rangle$  would not have a scaling behavior as in Eq.(17). For that reason we focus on the simple properties of  $S_q$ . The dependence of  $\sigma_q$  on  $q$  is shown in Fig. 7, where a remarkable linear behavior is found. We use the parameterization

$$\sigma_q = s_0 + s q \quad (18)$$

and find  $s = 0.76$ .

Among the quantities that are under our control in the analysis, we have studied the dependences on  $M$  and  $q$ . The remaining such quantity is  $\rho_0$ , while  $T$  is beyond experimental control, although it can be varied in the simulation. We now study the dependence of  $c$  and  $s$  on  $\rho_0$  and  $T$ , which are shown in Figs. 8 and 9. Evidently, at higher values of  $\rho_0$  the dependence on  $T$  are more pronounced than at  $\rho_0 = 20$ . Similar behavior has been found for  $c_0$  and  $s_0$ , defined in Eqs. (14) and (18). This result is very interesting, and provides a possible avenue toward learning more about the nature of PT in a realistic heavy-ion experiment.

If a quark-gluon plasma is formed in a heavy-ion collision, the expanding cylinder has high  $T$  in the interior and low  $T$  on the surface. Our modeling has been to investigate the properties of hadronization on the surface. Since the PT is a smooth cross-over in the neighborhood of  $T_c$ , and also since hydrodynamical flow can lead to local fluctuations in temperature and radial velocity on the surface, it is realistic to expect the hadrons to form in a small range of  $T$  around  $T_c$ , a possibility that cannot be controlled experimentally nor excluded theoretically. To learn whether the hadronization takes place over a range of  $T$ , we suggest on the basis of Figs. 8 and 9 to use  $\rho_0$  as a device to probe the properties of the PT.

In an analysis of the experimental data one can use a phenomenological density threshold to play the role of  $\rho_0$  and vary it in the determination of the patterns of voids. From our study we have learned that for a wide range of  $\rho_0$  the values of  $c$  and  $s$  are not independent of  $T$ . It means that if the PT occurs over a range of  $T$  so that the hadrons detected are formed at various  $T$  around  $T_c$  even within one event, then for  $\rho_0$  in that range of nonuniform  $c$  and  $s$  the dependences of  $\langle G_q \rangle$  and  $S_q$  on  $M$  would not exhibit simple power-law behavior as in Figs. 4 and 6, since nonuniform values of  $\gamma_q$  and  $\sigma_q$  for any  $q$  would lead to  $M$ -dependences that are not simple power-laws. If, by varying  $\rho_0$  to a point that corresponds to 20 in this study, simple scaling behaviors can be found for  $\langle G_q \rangle$  and  $S_q$  with  $c$  and  $s$  having roughly the values 0.8 and 0.76 respectively, then we can be assured that the PT is a cross-over of the type that we have studied here in the Ising model. The signature for having a unique  $T_c$  for hadronization is that the scaling behavior persists at any  $\rho_0$  and the lowest values of  $c$  and  $s$  are at 0.7 and 0.67, respectively, when  $\rho_0 = 50$ .

## 4 Configuration Mixing

The possibility of hadronization occurring at a narrow range of temperatures discussed at the end of the previous section is not the only complication that may occur in a heavy-ion collision process. A configuration that we simulate on the Ising lattice corresponds to the cluster and void pattern of one instant (with uncertainty 1 fm/c) in the hadronization history of a plasma cylinder. The final state of a collision process registered at the detector is a collection of all the particles produced throughout the whole evolution process in excess of 10 fm/c. The clusters and voids produced at different times overlap one another in the integration process, resulting in a smooth spatial distribution. Thus to identify the clustering patterns in an experiment, it is necessary to make cuts in the phase space. Since  $\eta$  and  $\phi$  are needed to exhibit the 2D patterns,  $p_T$  is the only remaining variable, in which cuts can be made. Since there is some correlation between  $p_T$  and the evolution time, the selection of particles having their  $p_T$  lying in a very narrow interval,  $\Delta p_T$ , has the effect of selecting a small interval,  $\Delta\tau$ , in evolution time [1]. However, the correspondence is not one-to-one. In every  $\Delta p_T$  interval, patches of hadrons produced at neighboring times can contribute. That is what we mean by configuration mixing: the experimental configuration detected in a small  $\Delta p_T$  interval may be a mixture of parts of configurations produced at different times, the latter being the pure configurations that we simulate on the Ising lattice.

To simulate a mixed configuration, we make the following choice for definiteness. We divide the lattice into four quadrants. In each of the quadrants we place the corresponding quadrant of a new and independent configuration so that the mixed configuration consists of four parts of four configurations. On  $5 \times 10^3$  such mixed configurations we then performed the same analysis as in the preceding section. The results are summarized in Figs. 10 and 11 where, for comparison, the straight lines are reproduced from those in Figs. 5 and 7 for the pure configurations. The squares are the results for  $\gamma_q$  and  $\sigma_q$  calculated from the mixed configurations. Evidently, configuration mixing does not introduce any discernible deviation from the results of the pure configurations. The agreement being so good, we see no point in trying out other ways of mixing. The implication of the result is remarkable, but not surprising. The cluster and void patterns fluctuate so much that it does not matter whether

some pieces of the patterns come from different configurations, provided that the appropriate measure of the fluctuations is extracted. What we have extracted is the scaling behavior in  $M$ . The scaling exponents are then found to be independent of the configuration mixing.

## 5 Conclusion

We have shown in this paper that the study of voids can be very fruitful in finding signals of quark-hadron phase transition in heavy-ion collisions. The use of 2D Ising model has been effective in simulating a cross-over in the hadronization process.  $G_q$  moments have been defined to quantify the dependence of the voids on the bin sizes. The scaling behavior that has been found provides an efficient way to use the scaling exponents  $\gamma_q$  and  $\sigma_q$  to characterize the properties of the phase transition.

The temperature at which hadronization occurs is not under experimental control. We have found a way to learn whether hadronization occurs at a range of  $T$  or at a unique  $T$ . That is achieved by varying the density threshold  $\rho_0$ . A bin whose average density is  $< \rho_0$  is identified as belonging to a void. The quantity  $\rho_0$  is under the control of the analyst of the experimental data. If by varying  $\rho_0$  one finds that a scaling behavior can be tuned out, i. e. the power-law dependence on  $M$  becomes invalid for a range of  $\rho_0$ , then hadronization does not occur at a unique  $T$ . On the other hand, if scaling remains manifest for a range of  $\rho_0$ , then there is only one temperature at which hadrons are formed.

Even in the case where hadronization takes place in a range of  $T$ , it is possible to tune  $\rho_0$  to a value where strict scaling can be observed. Then  $\gamma_q$  and  $\sigma_q$  provide the slope parameters  $c$  and  $s$  that can be checked as numerical constants characteristic of the cross-over PT. Since there are no numerical inputs in our analysis, the values  $c = 0.8$  and  $s = 0.76$  are predictions in this study. Experimental verification of those numbers would, of course, lend significant support to this line of study. If the experimental numbers for  $c$  and  $s$  turn out not to have those values, or if there is no scaling behavior at all, one could conclude that the hadrons are formed without the system having gone through a phase transition.

We have further found that the study of the scaling behavior of the void moments has the additional virtue of being independent of configuration mixing. That property strengthens the argument that a small  $\Delta p_T$  cut in the data can provide us with a window to look into the hadronization process at a small  $\Delta\tau$  time interval where hadron clusters and voids are formed. The effect of randomization by the possible hadron gas in the final state on the scaling behavior has already been found in [1] to be minimal. Thus, we have here a promising procedure to investigate the properties of quark-hadron phase transition that should be undertaken by the heavy-ion experiments.

### Acknowledgment

We are grateful to Z. Cao and Y.F. Wu for providing us with the original code on the Ising model. This work was supported, in part, by U. S. Department of Energy under Grant No. DE-FG03-96ER40972.



## References

- [1] R. C. Hwa and Y. F. Wu, Phys. Rev. C **60**, 054904 (1999).
- [2] J. J. Binney, M. J. Dowrick, A. J. Fisher, and M. E. J. Newman, *The Theory of Critical Phenomena* (Clarendon Press, Oxford, 1992).
- [3] R. C. Hwa and Q. H. Zhang, hep-ph/9912275, Phys. Rev. D (to be published).
- [4] R. Graham and H. Haken, Z. Physik **213**, 420 (1968); **237**, 31 (1970); V. DeGiorgio and M. Scully, Phys. Rev. A**2**, 1170 (1970); R. C. Hwa, Acta Physica Slovaca **49**, 201 (1999).
- [5] M. R. Young, Y. Qu, S. Singh and R. C. Hwa, Optics Comm. **105**, 325 (1994).
- [6] R. C. Hwa and M. T. Nazirov, Phys. Rev. Lett. **69**, 741 (1992)
- [7] Z. Cao, Y. Gao and R. C. Hwa, Z. Phys. C **72**, 661 (1996).
- [8] See C. DeTar in *Quark-Gluon Plasma 2*, edited by R. C. Hwa (World Scientific, Singapore, 1995).
- [9] See K. Rajagopal, *loc. cit.*
- [10] R. C. Hwa, Phys. Rev. D **41**, 1456 (1990).
- [11] U. Wolff, Phys. Rev. Lett. **62**, 361 (1989).
- [12] Z. Cao and R. C. Hwa, Phys. Rev. Lett. **75**, 1268 (1995); Phys. Rev. D **53**, 6608 (1996); *ibid* **54**, 6674 (1996); Phys. Rev. E **56**, 326 (1997).

## Figure Captions

- Fig. 1** Average hadron density (in units of  $\lambda$ ) versus temperature (in units of  $J/k_B$ )
- Fig. 2** Spatial pattern of a configuration on the 2D lattice at  $T_c$ . Open squares indicate voids and filled squares indicate hadrons with  $\rho_0 = 20$ .
- Fig. 3** Probability distributions of  $\ln G_q$  (with  $q = 6$ ) at two different  $T$ .
- Fig. 4** Scaling behavior of  $\langle G_q \rangle$  vs  $M$  at  $T_c$ .
- Fig. 5** The dependence of  $\gamma_q$  on  $q$ .
- Fig. 6** Scaling behavior of  $\langle S_q \rangle$  vs  $M$  at  $T_c$ .
- Fig. 7** The dependence of  $\sigma_q$  on  $q$ .
- Fig. 8** The dependences of the slope parameter  $c$  on  $\rho_0$  and  $T$ .
- Fig. 9** The dependences of the slope parameter  $s$  on  $\rho_0$  and  $T$ .
- Fig. 10** A comparison of  $\gamma_q$  between the mixed configurations (squares) and the pure configurations (straightline taken from Fig. 5).
- Fig. 11** A comparison of  $\sigma_q$  between the mixed configurations (squares) and the pure configurations (straightline taken from Fig. 7).

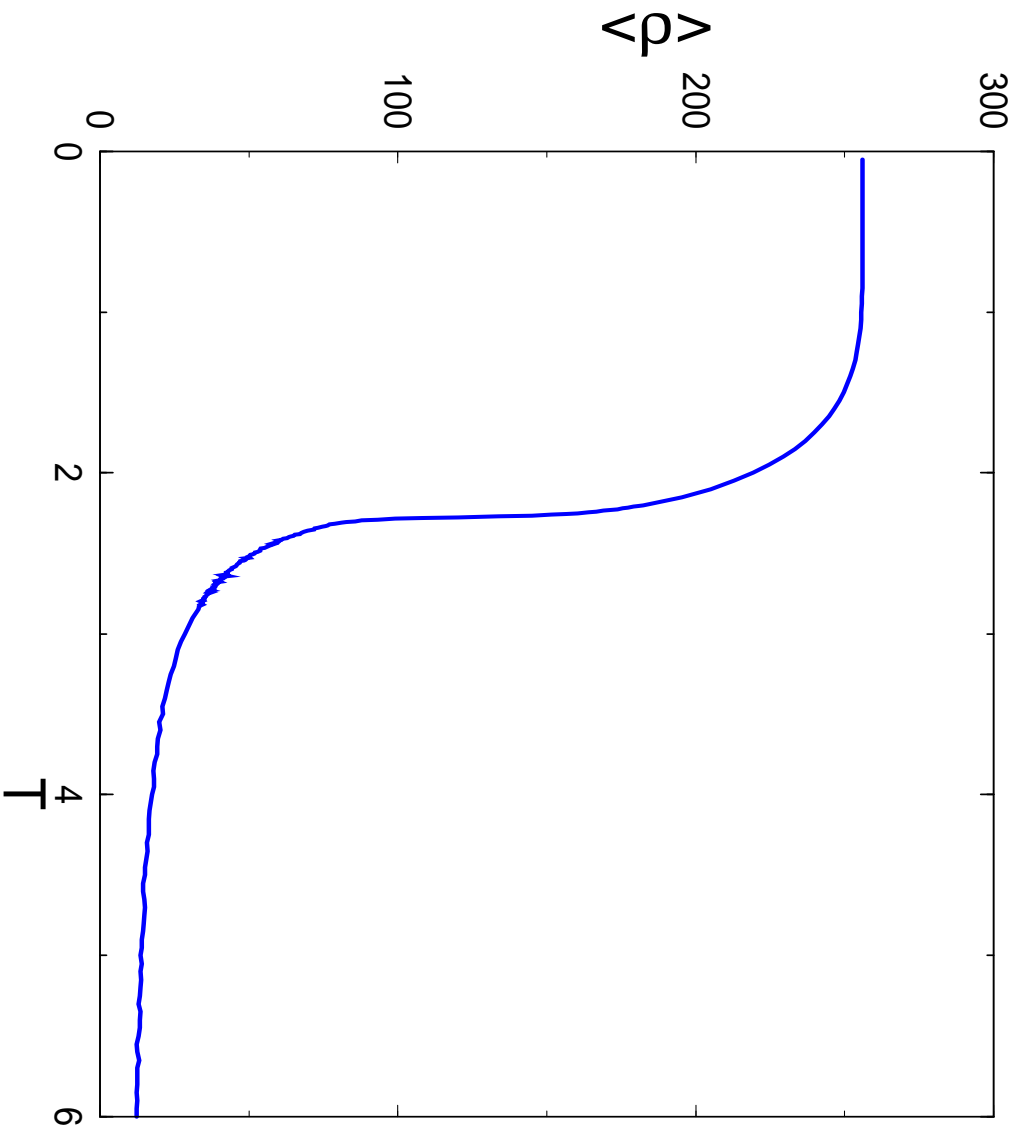


Fig. 1

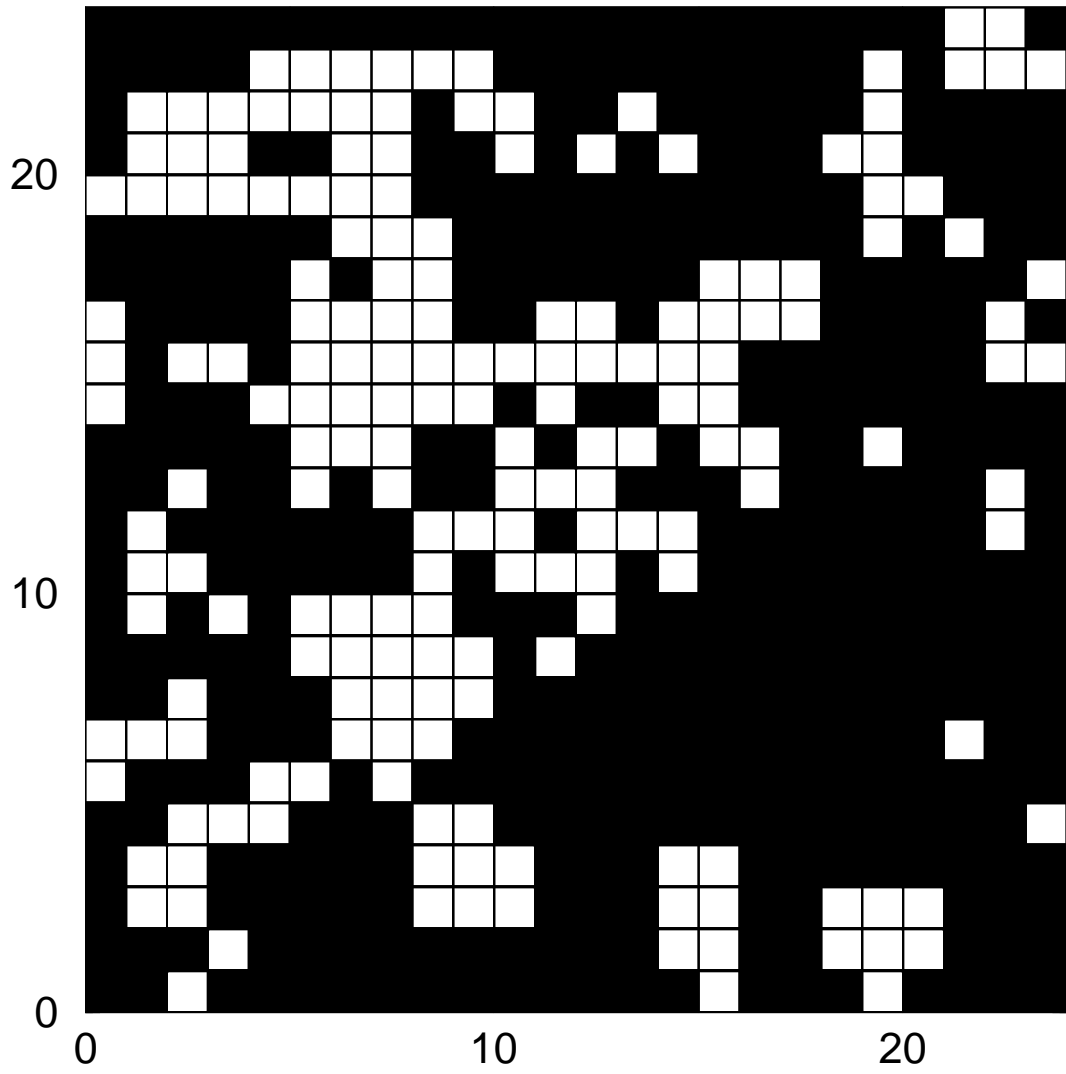


Fig.2

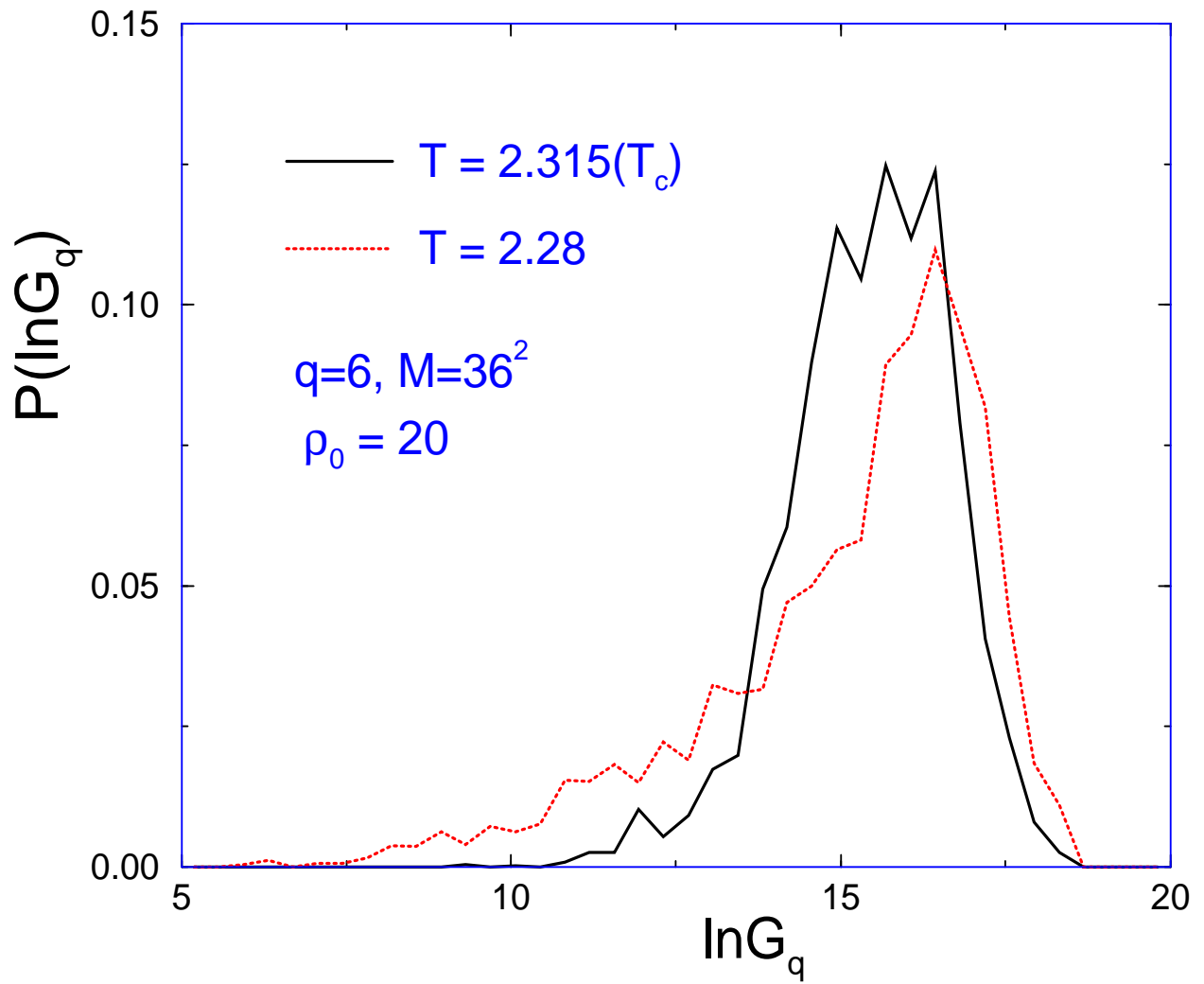


Fig.3

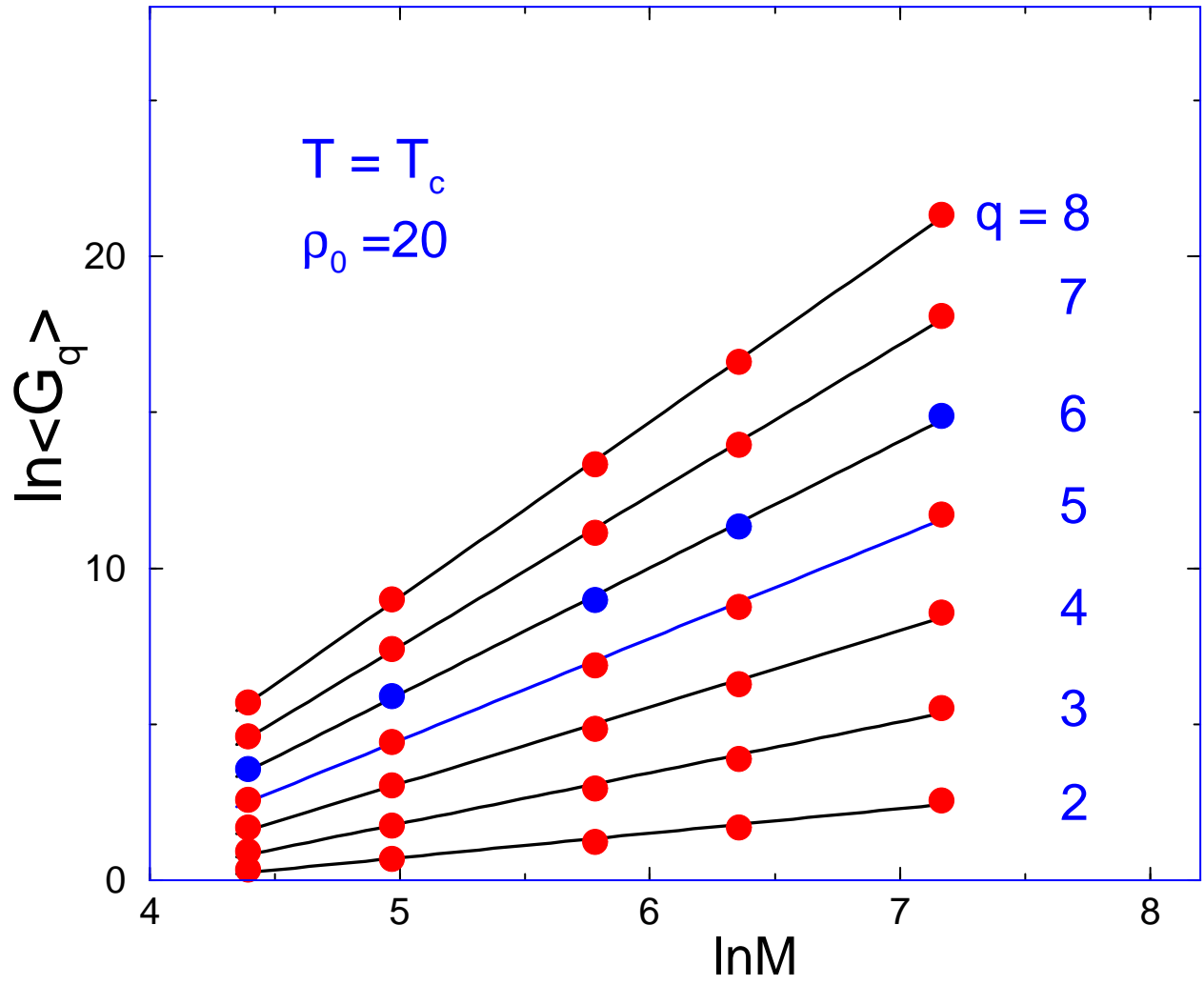


Fig.4

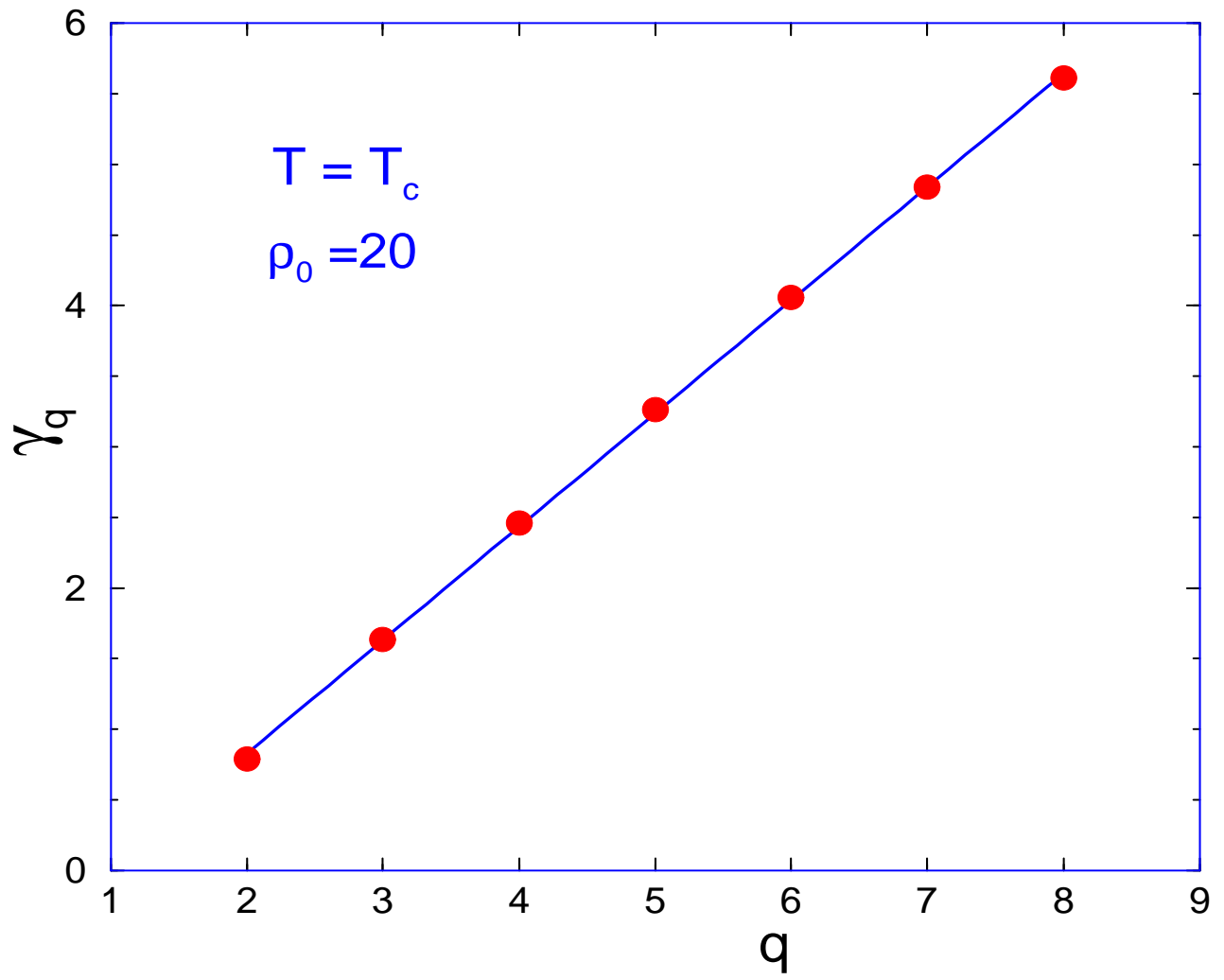


Fig.5

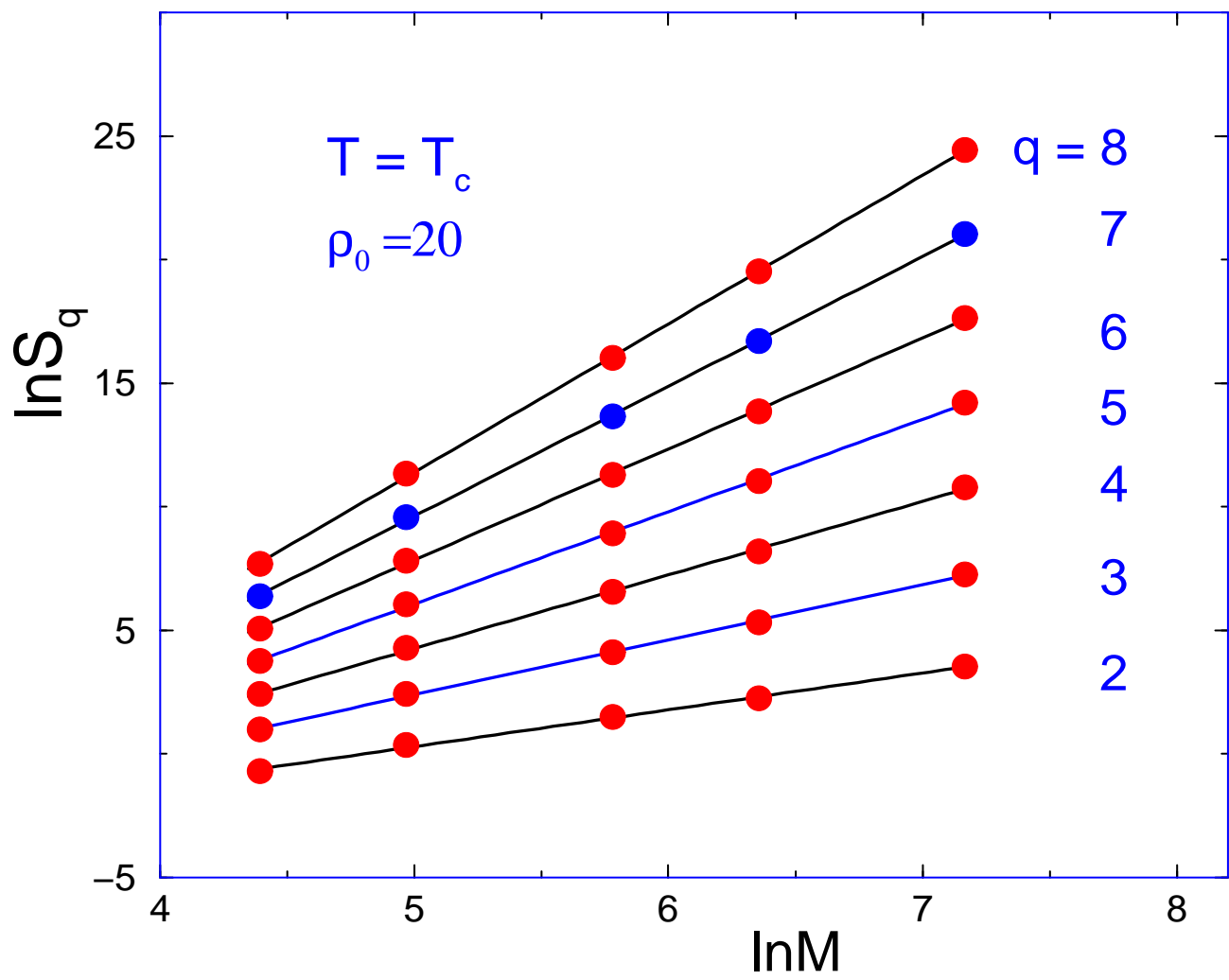


Fig.6



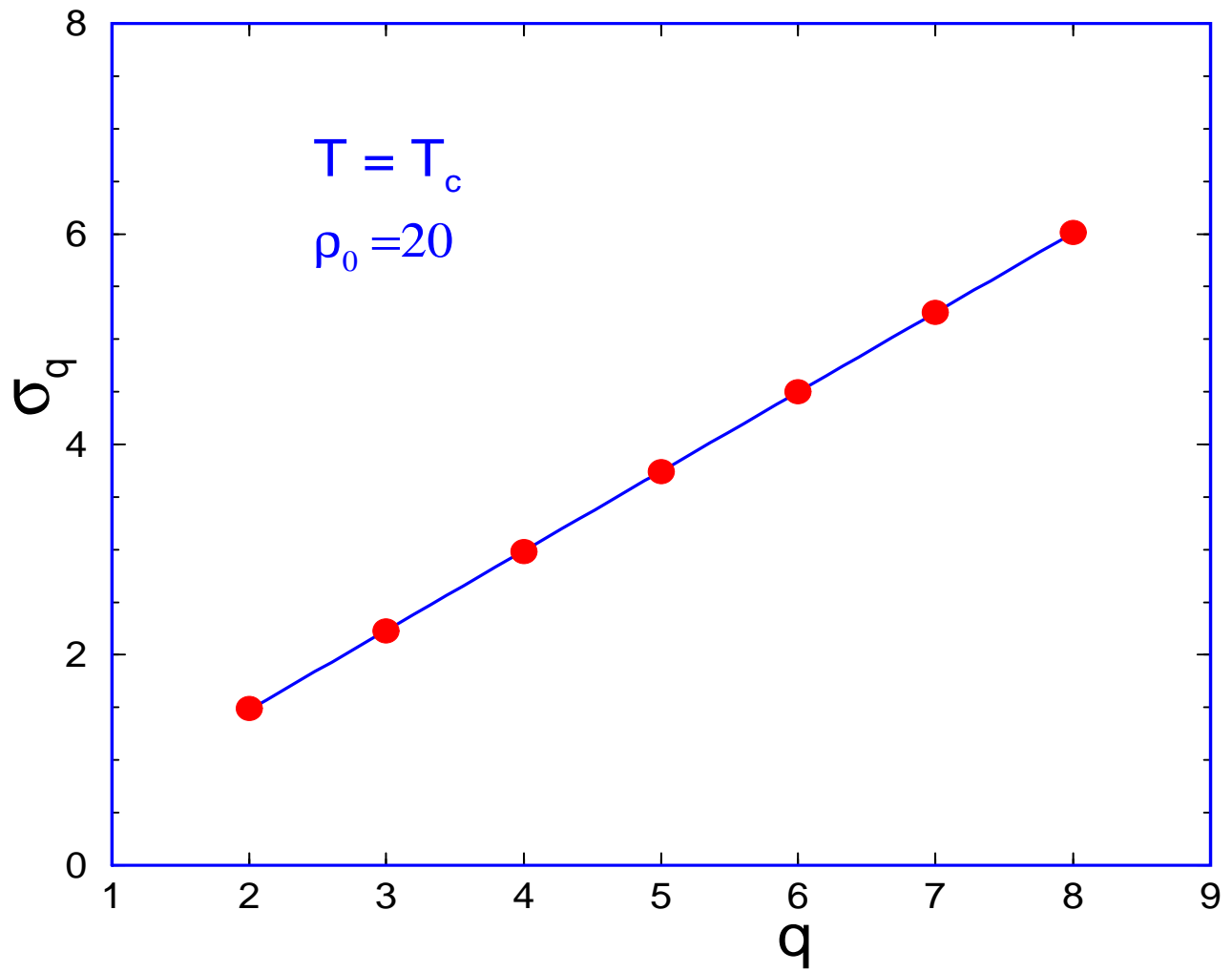


Fig.7

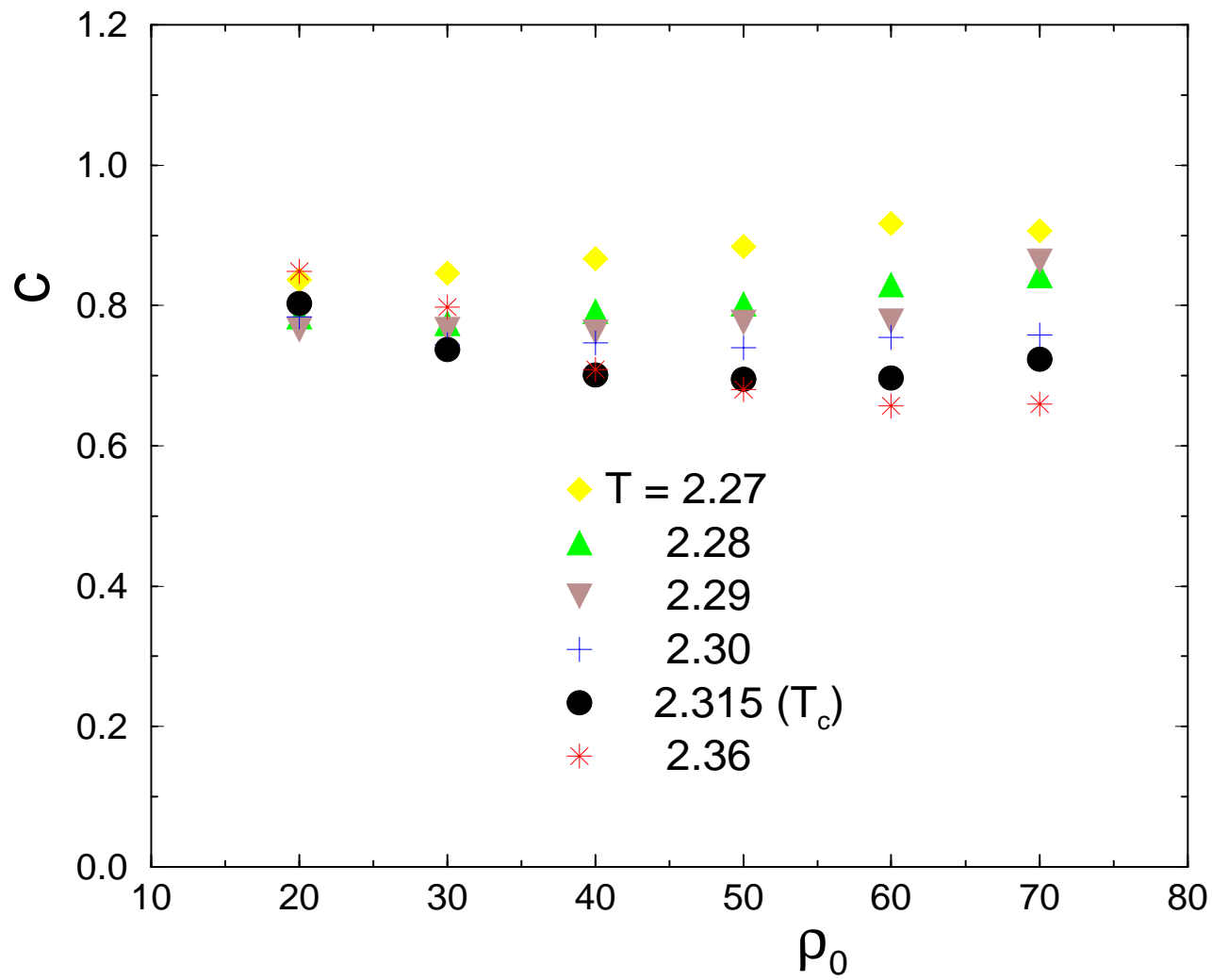


Fig.8

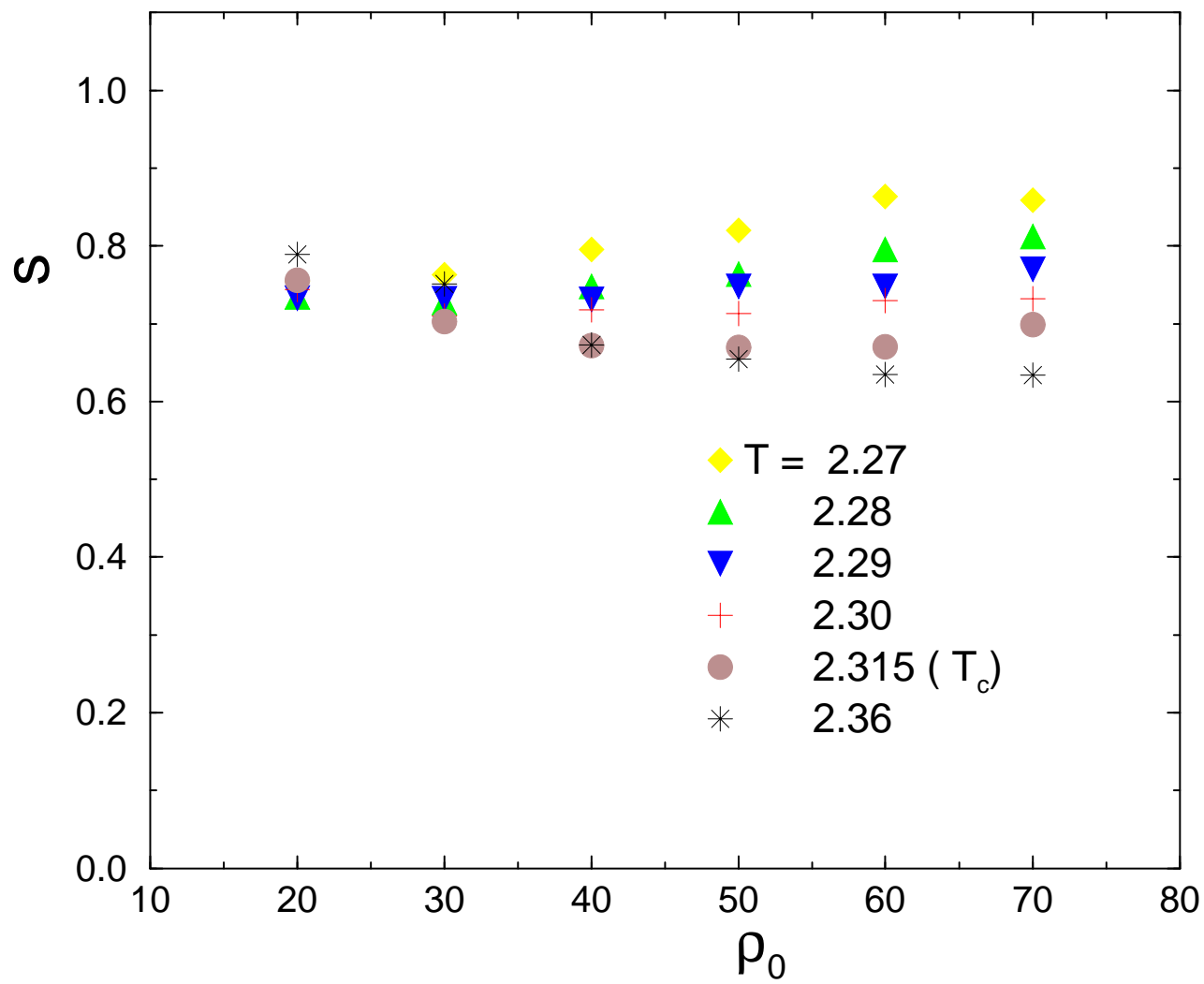


Fig.9

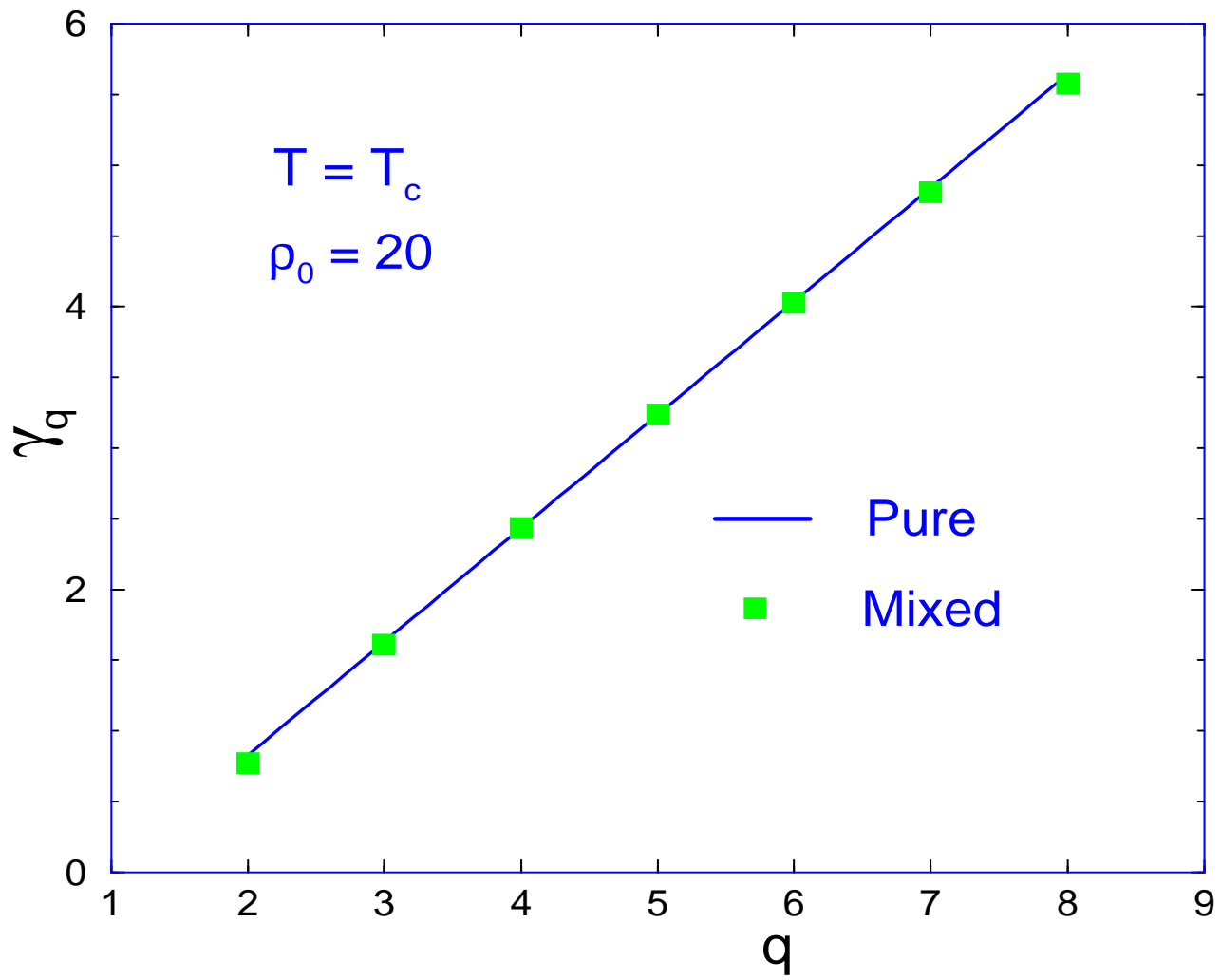


Fig.10

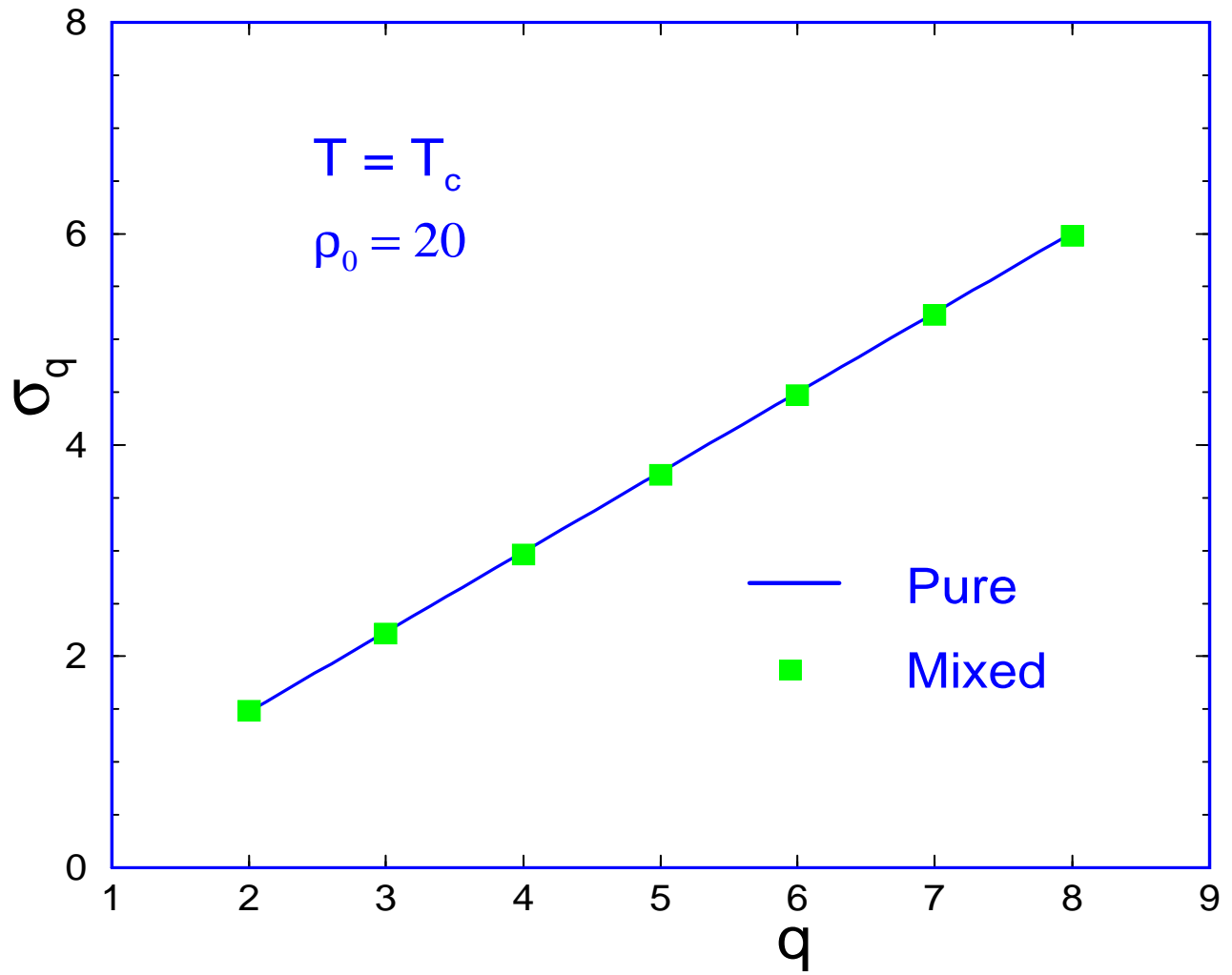


Fig.11